

PAPER • OPEN ACCESS

## Effects of phase angle setting, displacement, and eccentricity ratio based on determination of rhombic-drive primary geometrical parameters in beta-configuration Stirling engine

To cite this article: Z M Farid *et al* 2019 *IOP Conf. Ser.: Mater. Sci. Eng.* **469** 012047

View the [article online](#) for updates and enhancements.



**IOP | ebooks™**

Bringing you innovative digital publishing with leading voices to create your essential collection of books in STEM research.

Start exploring the collection - download the first chapter of every title for free.

# Effects of phase angle setting, displacement, and eccentricity ratio based on determination of rhombic-drive primary geometrical parameters in beta-configuration Stirling engine

Z M Farid<sup>1</sup>, A B Rosli<sup>1\*</sup> and K Kumaran<sup>1</sup>

<sup>1</sup>Faculty of Mechanical Engineering, Universiti Malaysia Pahang, 26600 Pekan, Pahang, Malaysia

\*Corresponding author: rosli@ump.edu.my

**Abstract.** Stirling engine is an external combustion engine, which generates power from any kind of heat source. Stirling engine offers lower emissions level compared to the internal combustion engines. The driving mechanisms differ based on the engine configurations. For beta-configuration Stirling engine, rhombic-drive mechanism indicates most suitable driving mechanism due to the concentric cylinder's arrangement. The determination of rhombic-drives primary geometrical parameters and consideration from various aspects are needed to achieve high power production, efficiency and ensure successful engine operation. In this paper, the kinematic investigations of rhombic-drives primary geometrical parameters are carried out to investigate the effects of phase angle, displacement and eccentricity ratio based on pre-determination of different crank offset radius, eccentricity ratio and connecting rod length. It is found that the adjustment of crank offset radius cause significant effect to the eccentricity ratio and engines displacement. Meanwhile, the adjustment of connecting rod length induced significant changes in phase angle since there are changes in TDC and BDC for both pistons.

## 1. Introduction

The continuation utilization of fossil fuel and associated environmental impact have leads to a growing interest in increasing and improving energy efficiency, as well as exploiting the renewable energy resources. The exploitation of renewable energy resources with useful low- and moderate-temperature heat source provides significant opportunities to the researchers and scientists for addressing the environmental issue and energy-related problem [1, 2].

The Stirling engine has draws an attention for recovering low- and moderate-temperature heat due to the great flexibility operating with any kind of heat source with potentially high efficiency. The attractive features such as simple mechanical constructions and usage of atmospheric air as working fluid provide a wide application prospect for recovering any low- and moderate-grade thermal energy [3-5]. Stirling engines can be classified into three common configurations; alpha-, beta-, and gamma-configuration. Each configuration has the same thermodynamic cycle but differ in mechanical design features. For beta-configuration Stirling engine, a displacer and power piston moves concentrically in the same cylinder, based on the movements of driving mechanism [6, 7].

Various driving mechanisms are adapted for the conversion of the thermal into mechanical energy. The driving mechanism varies by the engine configuration. Engine designers have developed suitable driving mechanisms to ensure high power output and efficiency [8]. For beta-configuration Stirling



engine, rhombic-drive mechanism indicates the most suitable as the displacer and power pistons move concentrically in the same cylinder, as shown in Figure 1. The usage of rhombic-drive mechanism offers advantages such as reduction of overall engine size, compact engine design, decrease the number of mechanical connections, and minimizing the decrease in efficiency due to friction and mechanical losses [8].

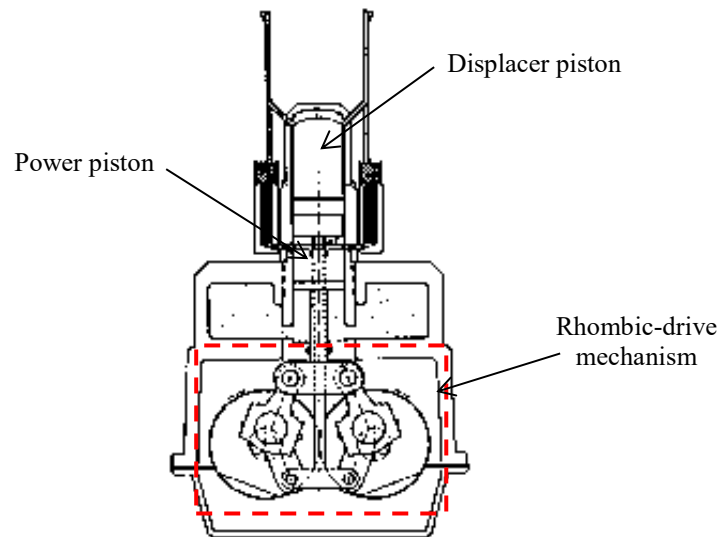


**Figure 1.** Beta-configuration Stirling engine with rhombic-drive mechanism [8].

Based on literature, the determination of geometrical parameters for driving mechanisms are crucial for achieving high power output and efficiency and to ensure successful engine operation. Various aspects have to be considered at different decision-making stages of the development of Stirling engine. For the present work, the kinematic investigations of rhombic-drives primary geometrical parameters are carried out within the design stage. The kinematic investigations focused on the changes of phase angle, engine stroke and eccentricity ratio based on different rhombic-drive primary geometrical parameters. For rhombic-drive mechanism, the determination of crank offset radius and connecting rod length with consideration of suitable eccentricity ratio and proper phase angle setting indicates important geometrical parameters [9].

## 2. Methodology

### 2.1. Kinematic relation of engine phase angle

Based on the working principle of Stirling engine, phase angle plays an important role in maximizing the engine power output. Lower phase angle setting can cause shorter heat transfer period for the contained working fluid to expand from the heat source and contract through the cooling source [10]. In order to determine the engine phase angle, the top dead centre (TDC) and bottom dead centre (BDC) crank angle position for both displacer and power piston are needed [9]. The trigonometric calculation starts with the determination of TDC and BDC crank angle position for both displacer and power piston based on 2D-schematic diagram as shown in Figure 2. Left-side Figure 2 shows the TDC position of the power piston, where the crank offset radius and the connecting rod are in one straight line and BDC position when the connecting rod covers the crank offset radius. Meanwhile, the right-side Figure 2 shows the displacer piston at TDC position when the connecting rod and the crank offset radius are in one straight line and BDC position when the connecting rod and crank offset radius are in collinear to each other.

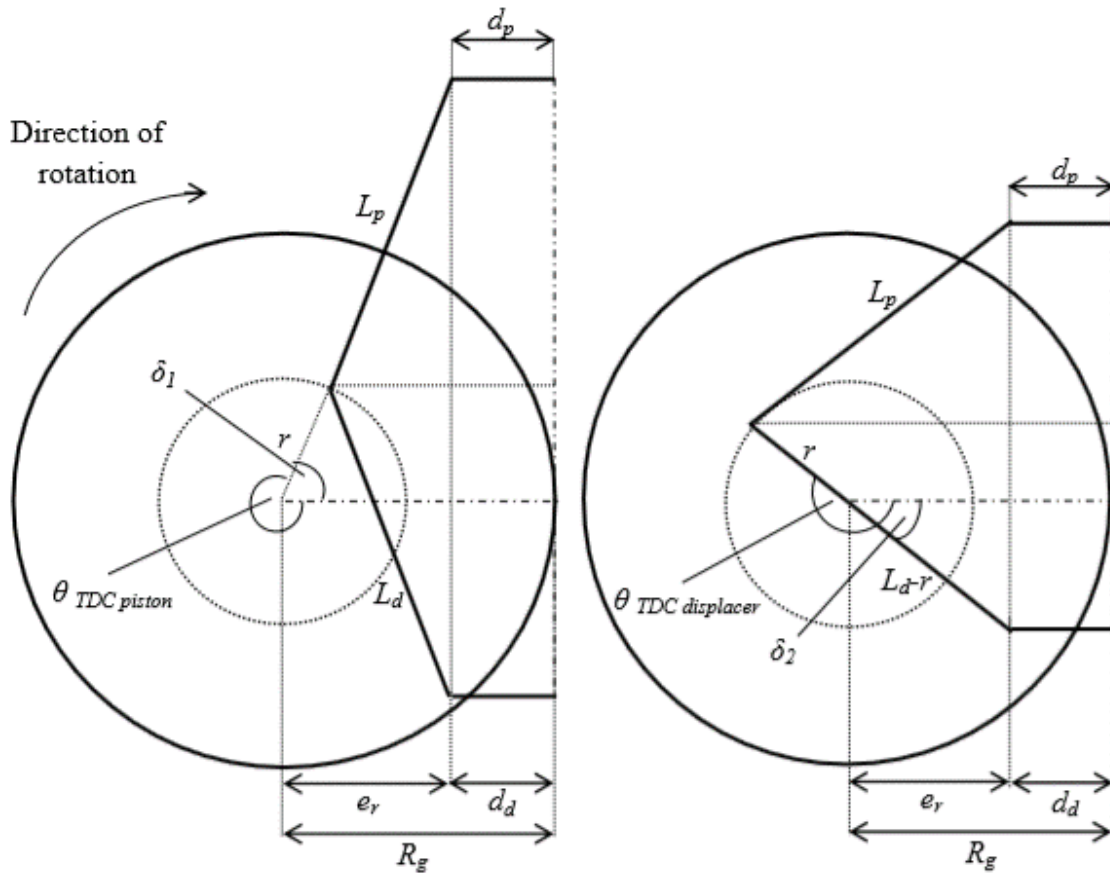


**Figure 2.** 2D-schematic of TDC positions for power piston (left) and displacer piston (right).

The phase angle can be determined by calculating the difference of crank angle between displacer and power piston TDC position. Therefore, the calculation begins by determining the crank angle,  $\theta$  of both displacer and power piston TDC position. From this calculation, the difference in motion between the displacer and power piston can be determined, as the displacer leads the power piston motion [9]. By considering the horizontal line as the crank angle's reference axis, the crank angle of the power piston TDC and BDC position can be determined. The crank offset angle for power piston TDC position is pre-determined by using the following equation (1):

$$\delta_1 = \cos^{-1} \left[ \frac{(R_g - d_p)}{(r + L_p)} \right] \quad (1)$$

Therefore, the crank angle for power piston at TDC and BDC position can be determined by using following equation (2) and (3):

$$\theta_{TDC \text{ piston}} = 360^\circ - \left[ \cos^{-1} \left[ \frac{(R_g - d_p)}{(r + L_p)} \right] \right] \quad (2)$$

$$\theta_{BDC \text{ piston}} = 180^\circ - \left[ \cos^{-1} \left[ \frac{(R_g - d_p)}{(L_p - r)} \right] \right] \quad (3)$$

Meanwhile, the crank offset angle for displacer piston TDC position, the equation (4) can be expressed as:

$$\delta_2 = \cos^{-1} \left[ \frac{(R_g - d_d)}{(L_d - r)} \right] \quad (4)$$

Therefore, the crank angle for displacer piston at TDC and BDC position can be calculated using following equation (5) and (6):

$$\theta_{TDC\ displacer} = 180^\circ + \left[ \cos^{-1} \left[ \frac{(R_g - d_d)}{(L_d - r)} \right] \right] \quad (5)$$

$$\theta_{BDC\ displacer} = \cos^{-1} \left[ \frac{(R_g - d_d)}{(r + L_d)} \right] \quad (6)$$

As a result, the phase angle difference can be determined by calculating the angle difference between the TDC position for both displacer and power piston, which is using following equation (7):

$$\alpha = \theta_{TDC\ piston} - \theta_{displacer} \quad (7)$$

The other rhombic-drives primary geometrical parameters such as spur gear radius,  $R$ , displacer and power piston's yoke radius,  $d$ , are based on the baseline of geometrical parameters proposed by [10]. Table 1 summarized the baseline and manipulated rhombic-drives primary geometrical parameters for the calculation of engine's phase angle.

**Table 1.** Rhombic-drives primary geometrical parameters.

Baseline parameters	Dimension (mm)
Spur gear radius, $R_g$	65
Displacer piston yoke radius, $d_d$	25
Power piston yoke radius, $d_p$	25
Manipulated parameters	Dimension (mm)
Crank offset radius, $r$	25-40
Displacer piston connecting rod, $L_d$	78-120
Power piston connecting rod, $L_p$	78-120

## 2.2. Determination of engine displacement/stroke

For the determination of engines displacement or stroke, the calculation can be performing based on the variations of rhombic-drives primary geometrical parameters. Within the principle of rhombic-drive, the displacement of both displacer and power pistons can be describe as equal, due to the symmetrical configuration about vertical axis, as shown in previous Figure 2. The displacer piston is in its lowest position when the connecting rod and crank offset are in one straight line. Then, its top position when the connecting rod covers the crank offset. In order to determine the engines displacement, the calculation can be calculated by using equation (8) [9]:

$$Stroke, S = \frac{r}{\lambda} \left[ ((1 + \lambda)^2 - (\lambda^2 \varepsilon^2))^{1/2} - ((1 - \lambda)^2 - (\lambda^2 \varepsilon^2))^{1/2} \right] \quad (8)$$

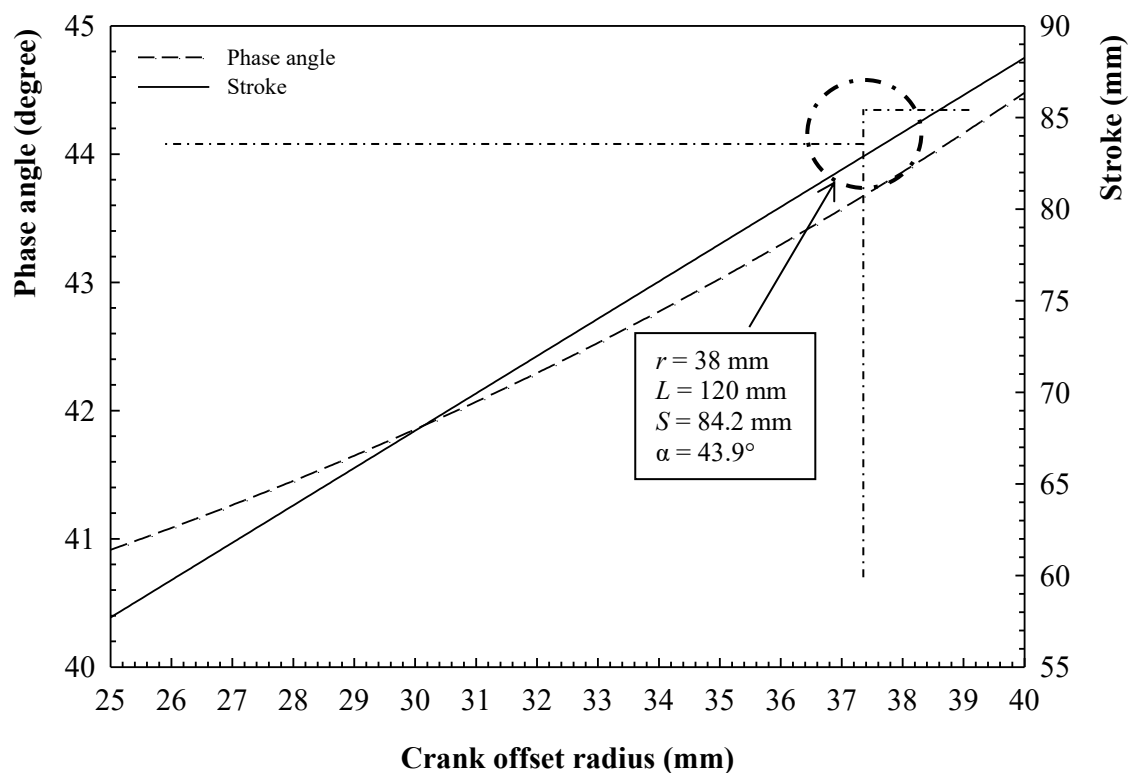
where the eccentricity ratio,  $\varepsilon$ ,

$$\varepsilon = \frac{e}{r}, \varepsilon > 1 \quad (9)$$

$$\lambda = \frac{r}{L}, (e + r) < L \quad (10)$$

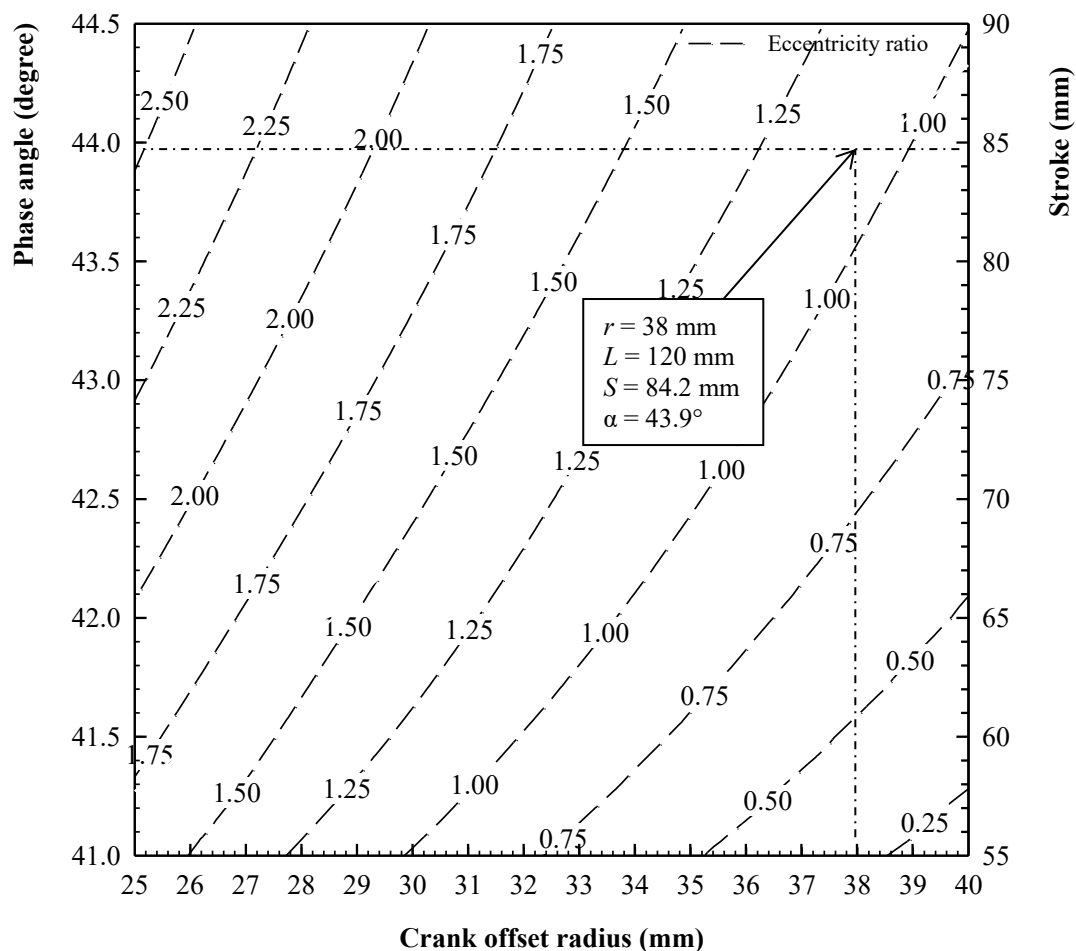
### 3. Results and discussions

Figure 3 shows the effect of engines phase angle and stroke at different crank offset radius based on the connecting rod length of 120 mm and crank offset radius of 38 mm proposed by [10]. The result indicates a minor change in engines phase angle within the adjustment of the crank offset radius. The engines phase angle varies from  $41^\circ$  to  $44.5^\circ$  with the variation of crank offset radius from 25 mm to 40 mm. Based on the engines phase angle calculation, the adjustment of crank offset radius does not give a significant effect to the engines TDC and BDC position, as well as the engines phase angle. However, the increase in crank offset radius shows higher engines displacement due to the increases in engines stroke. The engines stroke varies from 58mm to 88mm based on the variation of the crank offset radius from 25mm to 40 mm.



**Figure 3.** Effect of engine phase angle and stroke at different crank offset radius.

Meanwhile, the effect of engines phase angle, engine stroke and eccentricity ratio at different crank offset radius is shown in Figure 4. The result shows a significant variation in engines stroke and eccentricity ratio for different crank offset radius with baseline connecting rod length of 120 mm. The result indicates that as the crank offset radius increase, the eccentricity ratio decrease, based on the relation shown in Equation (9). Based on rhombic-drive working principle, the adjustment on crank offset radius does not give a significant change in engines phase angle, but only for eccentricity ratio [9]. Table 2 shows a sample of calculated data from different crank offset radius with connecting rod length of 120 mm.



**Figure 4.** Effect of engine phase angle, stroke, and eccentricity ratio at different crank offset radius.

**Table 2.** Sample of calculated data for different crank offset radius.

Crank offset radius, mm	Phase angle, °	Stroke, mm	Eccentricity ratio
25	40.9	57.7	1.60
30	41.6	67.9	1.33
35	43.9	84.2	1.05
40	44.5	88.3	1.00

The analysis of rhombic-drives primary geometrical parameters focused on the effect of engines phase angle and stroke at crank radius of 38 mm but different connecting rod length. Figure 5 shows the effect of engines phase angle and stroke at different connecting rod length, varies from 78 mm to 120 mm. The result shows that the engines phase angle varies from 44° to 110°. The figure indicates that the adjustment of connecting rod length has a significant influence to the engine TDC and BDC crank angle position for both displacer and power piston. However, the adjustment of connecting rod length indicates minor change in stroke, which varies from 84.20 mm to 89.40 mm. Meanwhile, the eccentricity ratio is found to be constant at any length of the connecting rod. The sample of calculated data is listed in Table 3.

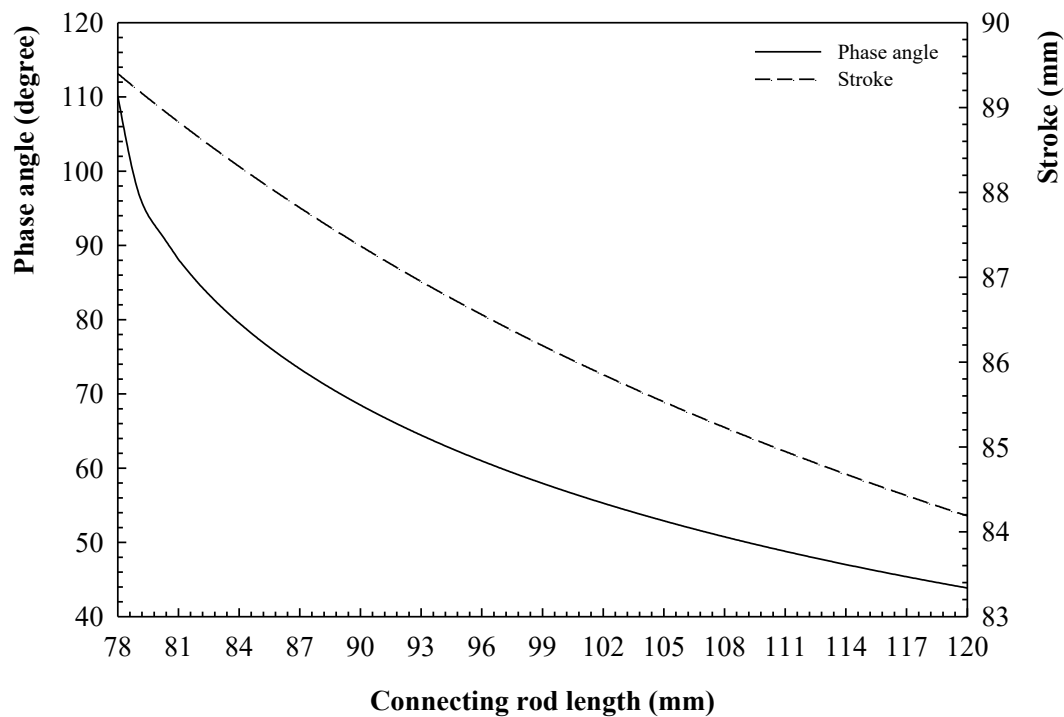


**Figure 5.** Effect of engine phase angle and stroke at different connecting rod length.

**Table 3.** Sample of calculated data for different connecting rod length.

Connecting rod length, mm	Phase angle, °	Stroke, mm	Eccentricity ratio
78	110.2	89.4	1.05
80.5	89.9	88.9	1.05
100	57.0	86.1	1.05
120	43.9	84.2	1.05

Figure 6 and 7 show the operation of rhombic-drive reciprocating displacement of the displacer and power piston based on the rhombic-drives primary geometrical parameters listed in Table 1. Figure 6 shows the displacer piston moves at  $90^\circ$  phase angle ahead of the power piston at crank radius,  $r = 38$  mm and connecting rod length,  $L = 80.5$  mm. Meanwhile, Figure 7 shows the displacer piston moves at  $74^\circ$  phase angle ahead of the power piston at crank radius,  $r = 30$  mm and connecting rod length,  $L = 80.5$  mm.

Based on two different  $r$  with same  $L$ , the value of  $r = 30$  mm as shown in Figure 6 provides smoother sinusoidal motion between crank interval from  $240^\circ$  to  $280^\circ$ , compared to the value of  $r = 38$  mm. The jerky motion occurrence between crank intervals from  $240^\circ$  to  $280^\circ$  in Figure 5 indicates that the crank radius and eccentricity ratio has a great influence to the operation of reciprocating displacement of both pistons. According to [9], the eccentricity ratio,  $\varepsilon$  usually lies between  $1 < \varepsilon < 2$  in order to avoid any jerky motion of linkage and excessive vibration. It can be controlled by selecting suitable crank radius, eccentricity ratio and connecting rod length. Therefore, the improper selection of  $r$  and  $\varepsilon$  can lead to the intermittent of driving mechanism, which causing unsuccessful engine operation.



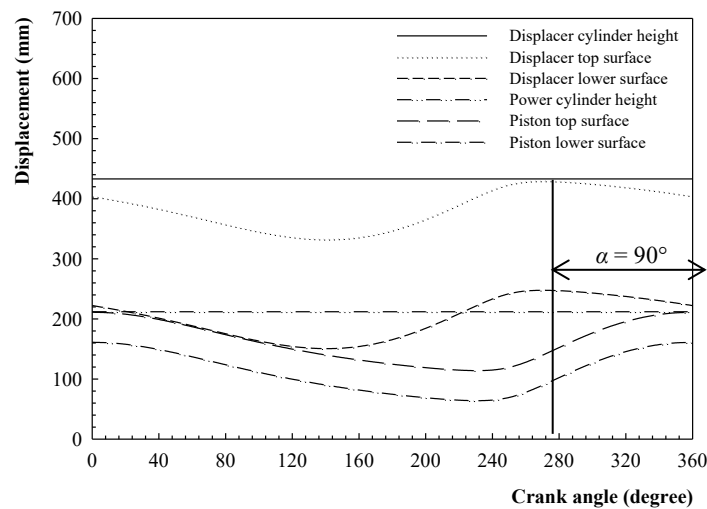


**Figure 6.** Reciprocating displacement of  $r = 38$  mm,  $L = 80.5$  mm

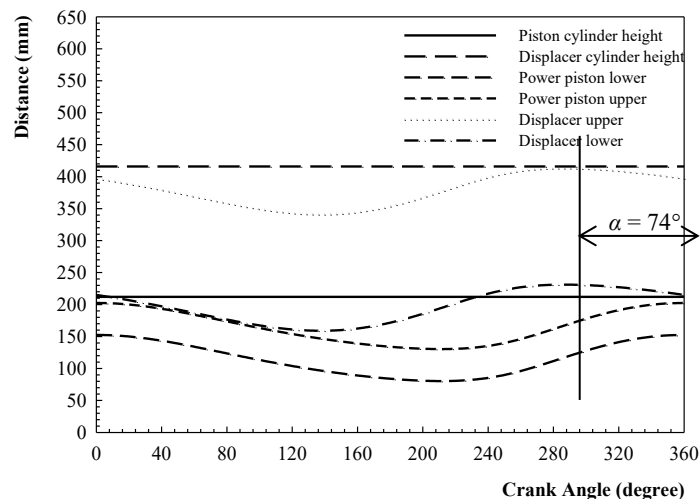


**Figure 7.** Reciprocating displacement of  $r = 30$  mm,  $L = 80.5$  mm

**Table 4.** Comparison of calculated data with different  $r$  with same  $L$ .

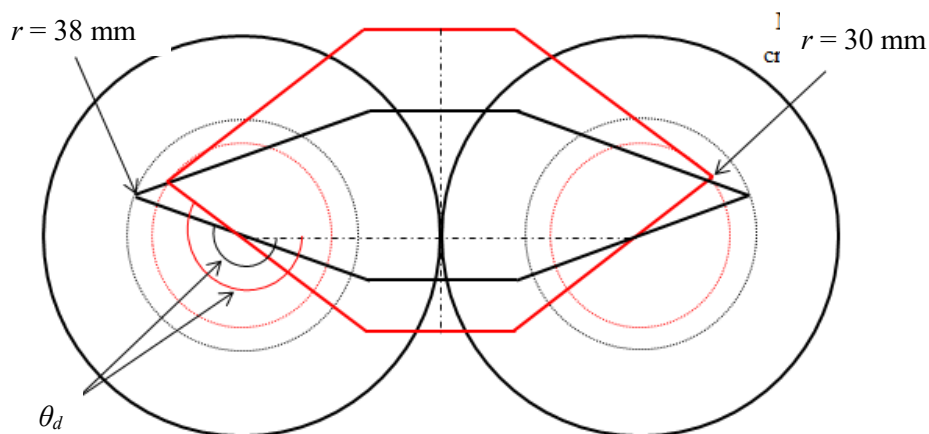
Crank offset radius, $r$ (mm)	Connecting rod length, $L$ (mm)	Eccentricity ratio, $\varepsilon$	Phase angle, $\alpha$ (degree)	Stroke, $S$ (mm)
38	80.5	1.053	89.98	88.92
30	80.5	1.333	73.60	72.38

Meanwhile, Figure 8 shows the TDC and BDC position for both displacer and power piston in comparison with two different  $r$  with same  $L$ . The comparison of TDC and BDC crank angle are listed in Table 4. The adjustment of  $r$  indicates significant changes for displacer TDC position, but minor changes for power piston TDC position. Indirectly, the phase angle between displacer and power piston will be different for both conditions. Table 5 summarized the comparison of eccentricity ratio, stroke, and phase angle based on two different crank offset radius with the same connecting rod length. Theoretically, a Stirling engine with a  $90^\circ$  phase angle indicates an optimum phase angle setting for

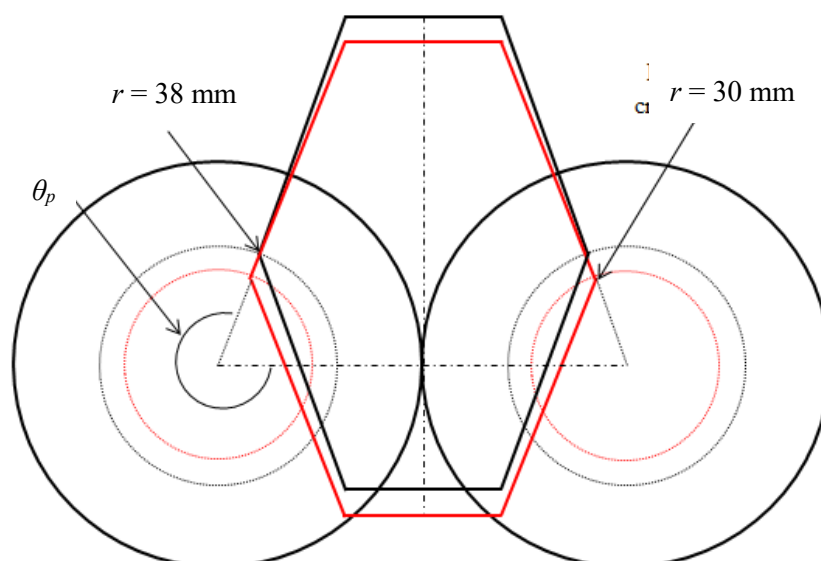
achieving highest power output [11]. In comparison of two different  $r$  with same  $L$ , the value of  $r = 38$  mm indicates optimum phase angle setting and higher engine displacement for achieving maximum power output. However, the jerky motion based on these geometrical parameters can lead to jerky motion of linkage during engine operation. As a result, the consideration of suitable crank radius, eccentricity ratio and proper phase angle setting must have taken into account while determining the proper geometrical parameters of the driving mechanism, specifically for rhombic-drive mechanism.

**Table 5.** Comparison of TDC and BDC.

Phase angle, $\alpha$	Crank angle, $\theta$ ( $^\circ$ )			
	Displacer		Power piston	
	TDC	BDC	TDC	BDC
90	199.75	70.27	289.73	160.25
74	217.62	68.78	291.22	142.38



(a) Displacer TDC position for  $r = 38$  mm (black line),  $r = 30$  mm (red line)



(b) Power piston TDC position for  $r = 38$  mm (black line),  $r = 30$  mm (red line)

**Figure 8.** TDC and BDC position for both displacer and power piston.

#### 4. Conclusions

In the design stage of Stirling engine, the determination of geometrical parameters for driving mechanism becomes an important step to ensure successful engine operation without any failure. Based on the kinematic investigations of rhombic-drives primary geometrical parameters, a proper selection of crank offset radius is critical since it has a great influence to the eccentricity ratio, however attributes to minor effect to the engine phase angle. The adjustment of connecting rod length indicates a significant effect to the engine phase angle, which influenced the TDC and BDC crank angle for both displacer and power piston. Despite of variation in crank offset radius, the adjustment of connecting rod length shows insignificant effect to the engine stroke. For rhombic-drive mechanism, the jerky motion of linkage and excessive vibration can be avoided by selecting suitable crank offset radius, eccentricity ratio and connecting rod length. However, further investigations on the thermodynamic performance of rhombic-drive beta-configuration Stirling engine based on the pre-determination of geometrical parameters are required before proceeding to the design and fabrications of engines mechanical components.

#### References

- [1] Wang K, Sanders S R, Dubey S, Choo F H and Duan F 2016 *Renew. and Sust. Energy Rev.* **62** 89-108
- [2] Yang H S and Cheng C H 2017 *Applied Energy* **200** 62-72
- [3] Hsu S T, Lin F Y and Chiou J S 2003 *Renewable Energy* **28** 59-69
- [4] Podesser E 1999 *Renewable Energy* **16** 1049-1052
- [5] Rokni M 2014 *Energy* **77** 6-18
- [6] Kongtragool B and Wongwises S 2003 *Renew. and Sust. Energy Rev.* **7** 131-154
- [7] Thombare D G and Verma S K 2008 *Renew. and Sust. Energy Rev.* **12** 1-38
- [8] Erol D, Yaman H and Dogan B 2017 *Renew. and Sust. Energy Rev.* **78** 1044-1067
- [9] Shendage D J, Kedare S B and Bapat S L 2011 *Renewable Energy* **36** 289-297
- [10] Ming G L 2012 *Development of Dish-Stirling concentrating solar thermal-electric energy conversion system* p 215-217
- [11] Sorea N and Cernomazu D 2009 *3<sup>rd</sup> International Symposium on Electrical Eng. and Energy Conver.*